Thermal conductance of interfaces between highly dissimilar materials

Ho-Ki Lyeo and David G. Cahill*
Department of Materials Science and Engineering and Frederick Seitz Materials Research Laboratory, University of Illinois, Urbana, Illinois 61801, USA
(Received 28 December 2005; published 3 April 2006)

The thermal conductance of interfaces between materials with low Debye temperatures (Pb or Bi) and dielectrics or semiconductors with high Debye temperatures (hydrogen-terminated Si, SiO_2, the native oxide of Be, sapphire, or hydrogen-terminated diamond) is measured using time-domain thermoreflectance. The interface thermal conductance G for these combinations of materials falls within a relatively narrow range, $8 < G < 30$ MW m^{-2} K^{-1}, at room temperature. Because the thermal conductance of interfaces with Bi, a semimetal, and interfaces with Pb, a metal, are similar, we conclude that the coupling of electrons in a metal to phonons in a dielectric substrate does not contribute significantly to the thermal transport at interfaces. For Pb or Bi on hydrogen-terminated diamond, the measured conductance greatly exceeds the radiation limit and decreases approximately linearly with decreasing temperature, suggesting that anharmonic processes dominate the transfer of thermal energy across interfaces between materials with highly dissimilar spectra of lattice vibrations.

DOI: 10.1103/PhysRevB.73.144301 PACS number(s): 66.70.+f, 65.40.−b, 66.90.+r, 68.60.Dv

I. INTRODUCTION

Recent developments of materials and devices with structures on nanometer length scales have created new opportunities and challenges in the science of thermal transport and the technology of thermal management. Interfaces play a particularly important role in the properties of nanoscale structures and nanostructured materials.[1] The thermal transport properties of an interface[2] are characterized by the thermal conductance per unit area G; G is the linear transport coefficient that relates the heat flux J at an interface to the temperature drop ΔT at the interface, $J = G\Delta T$.

In 1993 Stoner and Maris[3] reported measurements of the thermal conductance of a wide variety of interfaces and found a surprisingly narrow range of values, see Fig. 1. The largest thermal conductance at room temperature, for Al/Al_2O_3, was only a factor of 5 greater than the smallest conductance, for Pb/diamond, while the theoretical predictions for these two types of interfaces differ by more than a factor of 100. Recently, we extended the upper limit of the observed values of thermal conductance by preparing a structure, TiN/MgO, with a high degree of perfection on both sides of the interface; the MgO substrates are prepared by furnace annealing at 1400 °C and the TiN films are deposited by magnetron sputter deposition at 850 °C under clean conditions that produce nearly perfect epitaxial growth of TiN.[4] The thermal conductance was then in reasonably good agreement with the predictions of a diffuse-mismatch model that excludes heat transport by optical phonons. (Reddy and co-workers have recently emphasized the importance of using realistic phonon dispersions in calculations of the thermal conductance of interfaces at elevated temperatures.[5])

The subject of our present study is the lower limit of the conductance near room temperature. We expect low thermal conductance when the Debye temperature of the material on one side of the interface is much smaller than the Debye temperature of the material on the other side, e.g., Pb/diamond. In their 1993 study, Stoner and Maris[3] found a thermal conductance between Pb and diamond that was much larger than expected. The measured conductance, 30 MW m^{-2} K^{-1} at 298 K, is more than an order of magni-

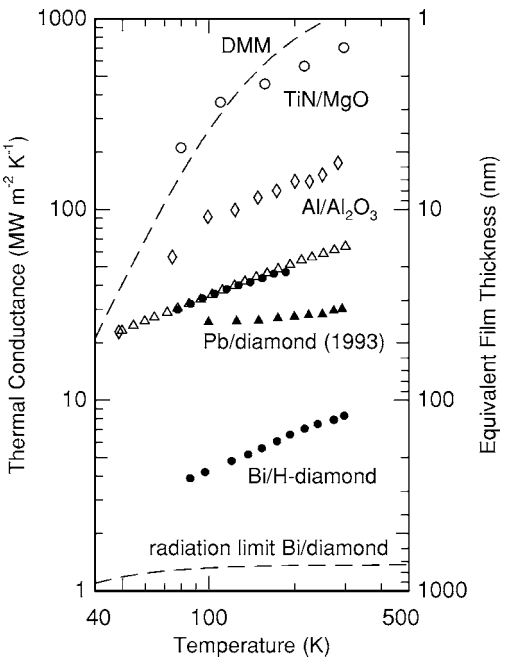

FIG. 1. Compilation of the thermal conductance of solid-solid interfaces. The right-hand axis gives the equivalent thickness of a thin film with a thermal conductivity of 1 W m^{-1} K^{-1} that has the same thermal resistance as these single interfaces. Data are taken from Ref. 4 (TiN/MgO, open circles); Ref. 3 (Al/Al_2O_3, open diamonds and Pb/diamond, filled triangles); Ref. 23 ($GST/ZnS:SiO_2$, open triangles); Ref. 24 (Al-oxide-Si structures, filled circles); and this work (Bi/hydrogen-terminated diamond, filled circles). The dashed-line labeled "DMM" is a theoretical calculation of the TiN/MgO interface conductance using a modification of the diffuse-mismatch model, see Ref. 4.

tude higher than the radiation limit, 2.5 MW m^{-2} K^{-1}; the radiation limit is the maximum possible conductance for transport by elastic processes involving two phonons, one phonon on each side of the interface.[3] Furthermore, the data for Pb/diamond were approximately independent of temperature between 100 and 250 K, see Fig. 1. These surprising results stimulated theoretical research on the possible causes of the anomalously large conductance.[3,6,7]

In this work, we obtain substantially different results for the thermal conductance of interfaces between materials with highly dissimilar vibrational spectra such as Pb or Bi and diamond. The most significant difference is that the thermal conductance decreases linearly with decreasing temperature. Thus, the anomalous contribution to the interface conductance becomes smaller at lower temperatures. Our experimental method, time-domain thermoreflectance, is essentially the same as the method used in Ref. 3 but, as we discuss in detail below, our method for data analysis provides higher dynamic range and greater sensitivity. We provide data for 13 combinations of interfaces with Pb and Bi at room temperature and report the temperature dependence of the data for 5 interfaces in the temperature range $80 < T < 298$ K.

II. EXPERIMENTAL DETAILS

A. Sample preparation

We deposit Pb and Bi films, ≈100 nm thick, on a variety of substrate materials with high Debye temperatures: Θ_D =550 K for SiO_2, 650 K for Si, 1000 K for sapphire, 1300 K for BeO, and 2200 K for diamond. The Debye temperatures of Pb and Bi are similar, 108 and 119 K, respectively. Hydrogen-terminated Si (denoted as H/Si in the discussion below) is prepared by pouring a 10% HF solution across both sides of a Si wafer for 5–10 s. We prepare thermally oxidized Si (denoted SiO_2/Si) by annealing H/Si at 850 °C for 3 min in air; the thickness of the oxide layer, typically 6 nm, is measured by optical ellipsometry. Sapphire substrates are cleaned by annealing at 850 °C in air for 15 min. Beryllium metal foils are cleaned by ultrasonication in acetone and methanol. The diamond substrates are cleaned in hot $HCl:HNO_3:H_2O$ (3:1:4) for 30 min and $H_2SO_4:HNO_3$ (6:4) for 20 min before terminating the surfaces with hydrogen by exposure to a hydrogen plasma for 30 min in a reactor at the University of Wisconsin.[8,9] We prepared "as-received" diamond substrates by rinsing in methanol. The diamond substrates are polished, large-grained, free-standing, polycrystalline films grown by chemical vapor deposition.

After preparation, each substrate is loaded into the deposition chamber; the chamber is then evacuated, baked at ≈165 °C for ~20 h, and allowed to cool to room temperature prior to depositing Pb or Bi. The Pb and Bi films are deposited by a thermal evaporation at a rate of >2 nm s^{-1}; the pressure in the chamber during depostion is $\approx 10^{-7}$ Torr. X-ray diffraction data show that the Pb and Bi films are strongly textured with the threefold axis normal to the surface. Pb films are fcc with (111) texture; the Bi films are most conveniently described by a six-atom hexagonal unit cell with (0001) texture.[10]

We are not aware of any studies of interface thermal conductance where the chemical purity or structural perfection of the interface has been well characterized. Our work with hydrogen-terminated Si and diamond are an attempt to control the chemical purity of the interfaces. Interfaces with diamond provide a unique opportunity to quantitatively measure oxygen contamination of the interface by Rutherford backscattering spectrometry (RBS) because ion scattering from oxygen at the buried interface can be clearly distinguished from ion scattering from Pb or Bi atoms of the film, or carbon atoms of the diamond substrate. Our motivation for using hydrogen-terminated diamond substrates was the hope that hydrogen-terminated diamond would provide a chemically cleaner interface for our experiments. RBS data confirmed this speculation: the oxygen contamination at the interface of the Pb/H/diamond samples is equivalent to the oxygen content of a 0.5 nm thick layer of PbO, whereas the contamination at the Pb/diamond interface is equivalent to a 2 nm thick layer of PbO. The oxygen contamination of the Bi/H/diamond interfaces are similar to the Pb/H/diamond interfaces.

B. Time-domain thermoreflectance

We measure the interface thermal conductance by time-domain thermoreflectance (TDTR) using a mode-locked Ti:sapphire laser that produces subpicosecond near-infrared pulses at a repetition rate of 80.6 MHz. The pump beam is modulated at 9.8 MHz by an electro-optic modulator; changes in the temperature of the metal film are monitored by changes in the intensity of a probe beam that is reflected from the surface. The small changes in the intensity of the reflected probe that are created by the pump beam are measured using a lock-in detection as a function of the delay time t between the pump and probe pulses. The $1/e^2$ radius of the focused pump and probe beams is 7 μm and the same power (≈5 mW) is used for both the pump and the probe at all temperatures. The reflectivity of Pb and Bi at 770 nm is ≈70% and 60%, respectively. In the worst case, sapphire substrates at 298 K, the steady-state temperature rise due to heat spreading in the substrate,[11] is ≈4 K. Each pulse of the pump or probe beam heats the Pb or Bi film by ≈2 K.

To a good approximation, the in-phase signal $V_{in}(t)$ of the rf lock-in amplifier is proportional to the time evolution of the temperature of the metal film. In most prior work using TDTR, only $V_{in}(t)$ is analyzed to extract the thermal properties of the sample.[3,12,13] This approach works well when the relaxation rate of the surface temperature is relatively fast; when the relaxation rate is slow, however, special care is needed to minimize systematic errors created by changes in the diameter of the focused pump or probe beam or changes in the spatial overlap of the pump and probe beams as the delay time is varied.[14]

These difficulties are illustrated in Fig. 2 where we analyze model calculations of a TDTR experiment for a metal film on a high thermal conductivity substrate using various values of the interface thermal conductance. These model

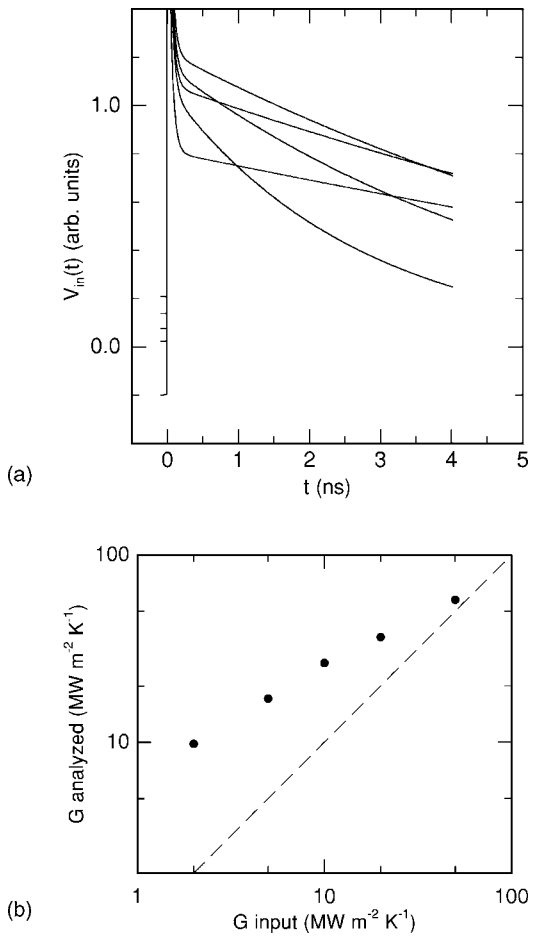

FIG. 2. (a) Calculations of the in-phase signal V_{in} of the lock-in amplifier as a function of delay time t between the pump and probe for various values of the interface conductance: $G=2$, 5, 10, 20, and 50 MW m^{-2} K^{-1} for the five curves. Each curve has been multiplied by a factor of $[1-0.06t/(1\ \text{ns})]$ to simulate changes in the signal that are created by changes in the diameter or overlap of the pump and probe beams. The metal film thickness is 100 nm. (b) Values of G extracted from an analysis of the simulated data are shown in (a). The analyzed values for G are plotted as a function of the value of G used as an input to the thermal model. The dashed line shows perfect agreement between the analyzed value for G and the input value for G.

calculations are essentially numerical simulations of the TDTR experiment and are based on an analytical solution of the heat diffusion equation in cylindrical coordinates for samples with any number of layers.[11] In our implementation of TDTR at the University of Illinois, the radius of the focused pump beam increases slightly with increasing delay time and this change in the beam radius produces an $\approx 6\%$ decrease in the lock-in signals for each ns increase of the delay time. We have included this factor in the curves plotted in Fig. 2(a). We then analyze the simulated data in Fig. 2(a) using the standard approach of (i) subtracting the baseline signal measured at negative delay time $t<0$; (ii) fitting the result to an exponential decay to determine a decay time-constant τ; and (iii) equating $G=hC/\tau$, where h is the metal film thickness, and C the heat capacity per unit volume of the metal film.[3] Values for G derived by this route are plotted as

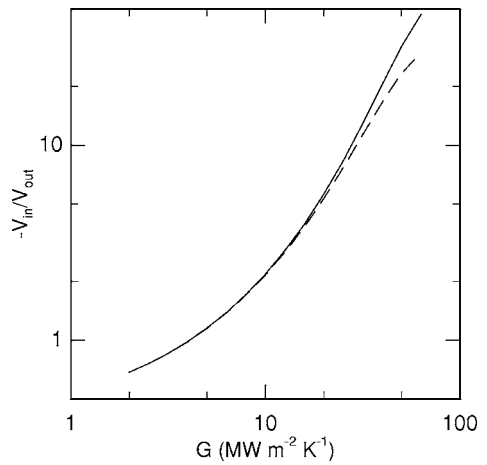

FIG. 3. Calculated values for the ratio of the in-phase and out-of-phase signals of the lock-in amplifier V_{in}/V_{out} at a delay time $t=1$ ns plotted as a function of the interface thermal conductance G. For this example, the metal film is Pb and the substrate has a thermal conductivity comparable to diamond (2000 W m^{-1} K^{-1}, plotted as a solid line) or a factor of 2 smaller (1000 W m^{-1} K^{-1}, plotted as a dashed line).

Fig. 2(b). We see that the standard approach works well when $G>40$ MW m^{-2} K^{-1} but becomes increasingly unreliable for smaller G.

The systematic errors in $V_{in}(t)$ described above can be reduced by expanding the beam that propagates through the variable delay stage, by using a much tighter focus for either the pump or probe,[12] or by sending the beam through an optical fiber after the delay stage.[14] We have developed a different approach;[4,11] we analyze the ratio V_{in}/V_{out} instead of $V_{in}(t)$ alone. This serves two purposes: changes in the radius or overlap of the pump and probe beams alter both V_{in} and V_{out} by a similar amount; and, furthermore, V_{out} is often more sensitive to the property of interest than $V_{in}(t)$. In Fig. 3, we plot simulations of the TDTR experiment and show that V_{in}/V_{out} has a steep dependence on G, steeper than linear, for $G>8$ MW m^{-2} K^{-1}. Therefore, measurements of V_{in}/V_{out} provide a highly sensitive measurement of G even when G is small.

Examples of measured TDTR data for three samples and fits to the data are shown in Fig. 4. The thermal model has one free parameter, the thermal conductance G of the interface, that is adjusted to obtain the best fit to the data at $t>1$ ns where the rate of heat transport in the Pb in Bi film is unimportant. The heat capacity of Pb and Bi is taken from literature values and the thicknesses of the metal layers are measured by picosecond acoustics.[15] The deviations between the fits and the data at short delay times, particularly pronounced for thick layers of Bi, is because our thermal model does not take into account rapid energy transport by nonequilibrium electrons and holes across distances much larger than the optical absorption depth.[16] For relatively thick Bi layers, the agreement between the fit and the data is also degraded by the uncertainty in the thermal conductivity of the Bi layer. We use bulk values for the thermal conductivity of Bi in our model but the thermal conductivity of the Bi film is presumably smaller than the bulk value. Nevertheless, as shown in

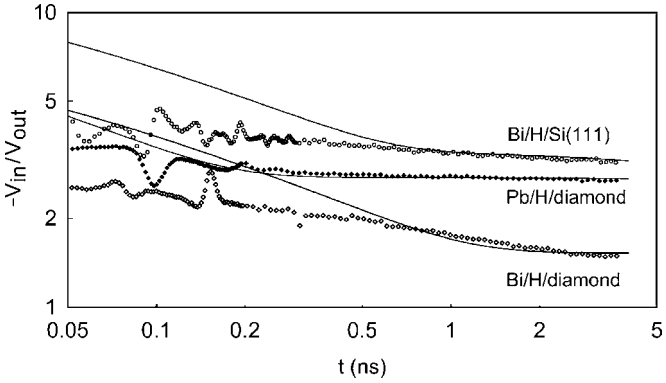

FIG. 4. Examples of time-domain thermoreflectance data measured at 298 K. The ratio of the in-phase to out-of-phase signals at the 9.8 MHz modulation frequency of the pump beam is plotted as a function of the delay time t between pump and probe. Solid lines are calculations with the thermal conductance of the interface adjusted to fit the data at $t>1$ ns. The disagreement at short times is because nonequilibrium electronic excitations distribute heat through the metal film in a manner that is not accounted for in the model. Peaks and valleys at short time delay are produced by longitudinal strain pulses that reflect from the surface and interface. Using sound velocities of 2.39 nm ps^{-1} and 1.97 nm ps^{-1} for Pb and Bi, respectively, the positions of these acoustic echoes give the thicknesses of the films: 89, 117, and 150 nm for Bi/H/Si, Pb/H/diamond, and Bi/H/diamond, respectively.

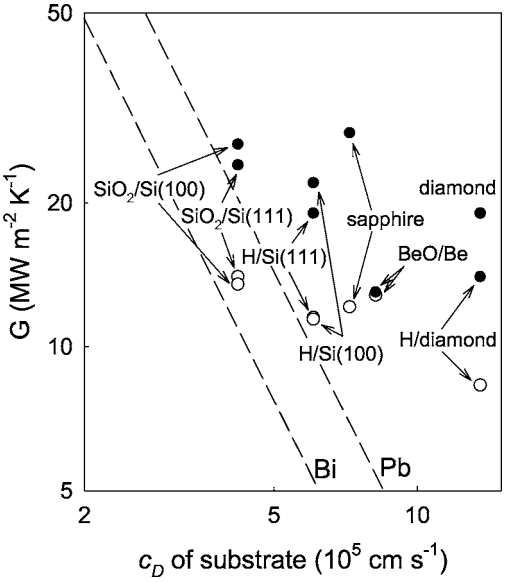

FIG. 5. Thermal conductance of Pb and Bi interfaces G measured at 298 K plotted as a function of the Debye velocity c_D of the substrates. Filled circles are data for Pb films deposited on labeled substrates and open circles are for Bi films. Dashed lines with a slope of −2 on this log-log plot are the radiation limits for the thermal conductance of interfaces with Pb and Bi, see Eq. (1). The maximum vibrational frequency $\nu_{\max}$ is 2.23 THz for Pb and 1.8 THz for acoustic modes in Bi, see Refs. 25 and 26.

Fig. 3, small deviations between the data and the thermal model do not lead to significant errors in the measurement of G. Even for the smallest values of G encountered in our work, the propagation of errors is no worse than a factor of ≈ 1.4; i.e., a 7% error in the fit of the model to the raw data produces less than a 10% error in the measurement of G. (We remind the reader that, in our approach, we fit the magnitude of V_{in}/V_{out} at long delay times, not the slope of V_{in} versus delay time.)

Because the interface is the controlling factor in the heat transfer, the data and the model calculations are relatively insensitive to the thermal conductivity and the heat capacity of the substrates. In other words, the accuracy of our measurements of the interface conductance is not dependent on the fact that the thermal conductivity of our polycrystalline diamond substrates is somewhat reduced by impurities and defects, see, for example, Fig. 3. A more subtle concern is the effect of changes in the phonon lifetime in the substrate on the thermal conductance. (Stoner and Maris used isotopically purified diamond films in their work; our diamond substrates have the natural isotope abundance.) The standard theoretical treatments do not consider this point but we have no reason to expect that small changes in phonon lifetimes will significantly alter the physics of vibrational energy transport at the interface.

III. RESULTS AND DISCUSSION

A. Room temperature data and the radiation limit

In Fig. 5, we compare the measured thermal conductance at 298 K to the theoretically predicted radiation limit. The phonon radiation limit is the maximum possible conductance produced by a purely harmonic process involving two phonons, one phonon on each side of the interface. To simplify this discussion, consider the specific case of Pb/diamond. The radiation limit for Pb/diamond is calculated by assuming phonons incident from diamond into Pb have a transmission coefficient of unity for all phonons in diamond with frequencies below the highest frequency vibrational mode of Pb, $\nu_{\max}$. The transmission coefficients are zero for phonons in diamond with frequencies greater than $\nu_{\max}$. The radiation limit is, therefore, a function of the cutoff vibrational frequency $\nu_{\max}$ of Pb (or Bi) and the Debye density of states in diamond (or the other high Debye temperature substrates).[3] At elevated temperatures, the radiation limit is independent of temperature and is given by

$$G_{rad} = \frac{\pi k_B \nu_{\max}^3}{c_D^2}, \tag{1}$$

where k_B is the Boltzmann constant. The Debye velocity c_D is defined by

$$\frac{3}{c_D^2} = \frac{1}{c_l^2} + \frac{2}{c_t^2}, \tag{2}$$

where c_l is the average longitudinal sound velocity, and c_t is the average transverse sound velocity. [Note that this definition of the Debye velocity is different than the definition used to calculate the Debye heat capacity; for heat capacity calculations, the second power of the sound velocities in Eq. (2) is replaced by the third power.] The thermal conductance

of interfaces with Pb and Bi exceed the radiation limit in all cases and the discrepancy between the data and the prediction increases as c_D for the substrate becomes larger.

We are aware of attempts to explain the unexpectedly large conductance of Pb/diamond interfaces by an electronic contribution.[6,7] Our data for Bi and Pb films are within a factor of 2 of each other for all substrates. We can consider the relative importance of electronic contributions to the thermal transport by comparing the electronic heat capacities of Bi and Pb. Since the Fermi energy of Bi is comparable to k_BT at 298 K, the electronic heat capacity of Bi will be approximately equal to the classical value, $(\frac{3}{2})k_B(N_e+N_h)$, where the electron and hole densities[17,18] at 298 K are $N_e=N_h\approx 2\times 10^{18}$ cm^{-3}. The electronic contribution to the heat capacity of Bi is therefore on the order of 8×10^{-5} J cm^{-3} K^{-1}. The heat capacity of Pb, a degenerate metal, is $\gamma_{Pb}T\approx 0.05$ J cm^{-3} K^{-1}, a factor of 600 larger than Bi. If an electronic contribution dominates the thermal transport for Pb interfaces, then the conductance of Bi and Pb interfaces should be vastly different. Since the conductance of Bi and Pb interfaces are similar, we conclude that an electronic contribution is unimportant.

Figure 5 includes data for interfaces with SiO_2 thermally grown on both (111) and (001) oriented Si wafers. We expect that the surfaces of these amorphous SiO_2 layers are essentially identical; therefore, the small differences in the conductance measured using SiO_2/Si(111) and SiO_2/Si(100) substrates can be taken as a measure of the reproducibility of our experiments. The morphology of hydrogen-terminated silicon, on the other hand, is known to depend on crystalline orientation:[19] hydrogen-terminated Si(111) is typically much smoother than Si(100). The thermal conductance, however, does not appear to be sensitive to these differences in morphology. The conductance of Bi/H/Si(100), see Fig. 5, is slightly higher than Bi/H/Si(111) but the conductance of Pb/H/Si(100) and Pb/H/Si(111) are nearly identical.

B. Temperature dependence of the interface thermal conductance

Recently, classical molecular dynamics (MD) simulations of the thermal conductance of model interfaces between two fcc crystals have revealed a significant temperature dependence; this temperature dependence was interpreted in terms of an inelastic scattering of phonons at the interface.[20] Using parameters appropriate for Pb/diamond, the MD simulations gave a conductance that decreased by a factor of 2.4 as the temperature was decreased from 300 to 100 K.

Our data for the temperature dependence of G for five selected interfaces are shown as Fig. 6. We observe a significant temperature dependence of the thermal conductance in all cases. The conductance of Pb/H/Si and Bi/H/Si interfaces closely approaches the radiation limit at $T<150$ K; the conductance of Pb/diamond, Pb/H/diamond, and Bi/H/diamond decreases approximately linearly with decreasing temperature. This linear temperature dependence of the excess thermal conductance is consistent with the MD simulations of Ref. 20 and suggests that anharmonicity plays an important role in heat transport across these interfaces.

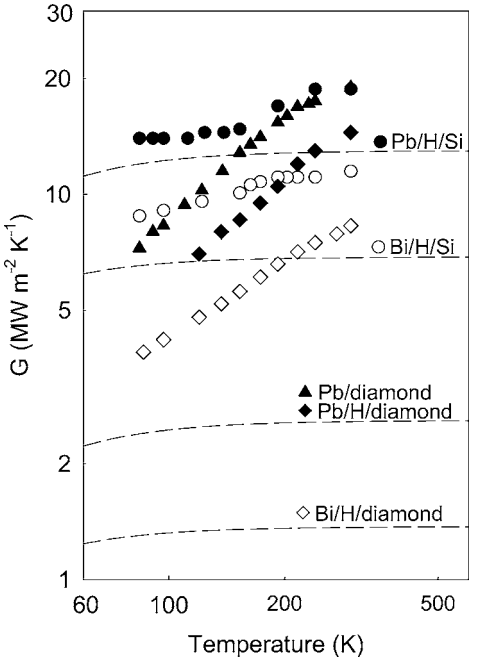

FIG. 6. Thermal conductance of selected interfaces plotted as a function of the measurement temperature. Filled symbols (circles, triangles, and diamonds) are data for Pb films on H/Si(111), diamond, and H/diamond, respectively; open symbols (circles and diamonds) are for Bi films on H/Si(111) and H/diamond. Dashed lines are calculations of the radiation limits, see Eq. (1).

One example of an anharmonic process that couples one phonon in diamond and two phonons in Pb or Bi is illustrated in Fig. 7; this example conserves both energy and crystal momenta and is reminiscent of the so-called "Klemens process" for the interaction between two acoustic phonons and an optical phonon near the center of the Brillouin zone.[21] Presumably, many combinations of frequencies

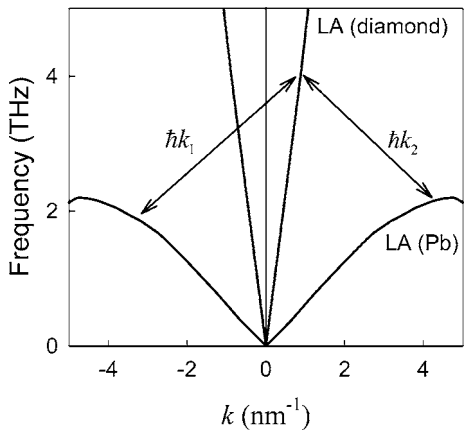

FIG. 7. Schematic illustration of one of many possible three-phonon processes that could contribute to heat transport at an interface between diamond and Pb. The curve labeled "LA (diamond)" is the dispersion of the longitudinal acoustic mode of diamond, see Ref. 27; and the curve labeled "LA (Pb)" is the dispersion of the longitudinal acoustic mode of Pb, see Ref. 25. Note that the arrows point in both directions because the process occurs near equilibrium.

and mode polarizations could contribute to the thermal transport in a similar manner.[22] (The focus of our research is experimental and a quantitative accounting of these various processes is beyond the scope of this work.) Since an elastic two-phonon process produces a thermal conductance that is approximately independent of temperature at $T > 50$ K, we can expect that three-phonon processes of the type depicted in Fig. 7 will contribute a channel to the thermal conductance that increases linearly with temperature for $T > 100$ K.

The conductance of interfaces formed by Pb deposited on diamond without further processing is $\approx 50\%$ higher than that of Pb deposited on hydrogen-terminated diamond, see Figs. 5 and 6. The larger oxygen contamination of the Pb/diamond interface relative to the Pb/H/diamond interface may play a role in this difference by altering the vibrational density of states near the interface.[20] Alternatively, the differences may be intrinsic: the hydrogen termination may directly modify the coupling between phonons in diamond and phonons in Pb. Since the lattice vibrations in Pb are fully thermally excited near room temperature, classical molecular dynamics simulations of interfacial heat transfer may provide useful insights on the sensitivity of the thermal conductance to disorder, chemical impurities, or degree of hydrogen termination.

In conclusion, we have identified that interfaces of Bi with hydrogen-terminated diamond have an extremely low thermal conductance of 8.5 MW m^{-2} K^{-1}. The thermal resistance of a single interface of this type has the same thermal resistance as a 100 nm thick layer of amorphous SiO_2. Nevertheless, the conductance greatly exceeds the radiation limit, i.e., the theoretical upper limit for an interfacial thermal transport that involves two phonons. The linear temperature dependence of the excess conductance suggests that three-phonon processes contribute a significant additional channel for the transport of heat between materials with highly dissimilar spectra of lattice vibrations.[20]

ACKNOWLEDGMENTS

The authors thank Wensha Yang and R. Hamers of the University of WI for preparing hydrogen-terminated diamond; Xuan Zheng and Zengbin Ge for their help with the experiments; Fumiya Watanabe for reviewing the manuscript; and D. Dlott for helpful discussions on vibrational energy transport. This work was supported by NSF Grant No. CTS-0319235 and DOE Grant No. DEFG02-01ER45938.

*Electronic address: d-cahill@uiuc.edu

[1] D. G. Cahill, W. K. Ford, K. E. Goodson, G. D. Mahan, A. Majumdar, H. J. Maris, R. Merlin, and S. R. Phillpot, J. Appl. Phys. **93**, 793 (2003).
[2] E. T. Swartz and R. O. Pohl, Rev. Mod. Phys. **61**, 605 (1989).
[3] R. J. Stoner and H. J. Maris, Phys. Rev. B **48**, 16373 (1993).
[4] R. M. Costescu, M. A. Wall, and D. G. Cahill, Phys. Rev. B **67**, 054302 (2003).
[5] P. Reddy, K. Castelino, and A. Majumdar, Appl. Phys. Lett. **87**, 211908 (2005).
[6] A. V. Sergeev, Phys. Rev. B **58**, R10199 (1998).
[7] M. L. Huberman and A. W. Overhauser, Phys. Rev. B **50**, 2865 (1994).
[8] T. Strother, T. Knickerbocker, J. N. Russell, Jr., J. E. Butler, L. M. Smith, and R. J. Hamers, Langmuir **18**, 968 (2002).
[9] W. Yang, J. E. Butler, J. John, N. Russell, and R. J. Hamers, Langmuir **20**, 6778 (2004).
[10] D. Schiferl and C. S. Barrett, J. Appl. Crystallogr. **2**, 30 (1969).
[11] D. G. Cahill, Rev. Sci. Instrum. **75**, 5119 (2004).
[12] R. J. Stevens, J. Heat Transfer **127**, 315 (2005).
[13] N. Taketoshi, T. Baba, and A. Ono, Jpn. J. Appl. Phys., Part 2 **38**, L1268 (1999).
[14] W. S. Capinski and H. J. Maris, Rev. Sci. Instrum. **67**, 2720 (1996).
[15] H. T. Grahn, H. J. Maris, and J. Tauc, IEEE J. Quantum Electron. **25**, 2562 (1989).
[16] G. Tas and H. J. Maris, Phys. Rev. B **49**, 15046 (1994).
[17] H. K. Collan, M. Krusius, and G. R. Pickett, Phys. Rev. Lett. **23**, 11 (1969).
[18] B. Abeles and S. Meiboom, Phys. Rev. **101**, 544 (1956).
[19] K. Endo, K. Arima, K. Hirose, T. Kataoka, and Y. Mori, J. Appl. Phys. **91**, 4065 (2002).
[20] R. J. Stevens, P. M. Norris, and L. V. Zhigilei, in *2004 ASME International Mechanical Engineering Congress and Exposition* (ASME, New York, 2004), pp. 37–46.
[21] P. G. Klemens, Phys. Rev. **148**, 845 (1966).
[22] A. Debernardi, S. Baroni, and E. Molinari, Phys. Rev. Lett. **75**, 1819 (1995).
[23] E.-K. Kim, S.-I. Kwun, S.-M. Lee, H. Seo, and J.-G. Yoon, Appl. Phys. Lett. **76**, 3864 (2000).
[24] D. G. Cahill, A. Bullen, and S.-M. Lee, High Temp. - High Press. **32**, 135 (2000).
[25] B. N. Brockhouse, T. Arase, G. Caglioti, K. R. Rao, and A. D. B. Woods, Phys. Rev. **128**, 1099 (1962).
[26] J. L. Yarnell, J. L. Warren, R. G. Wenzel, and S. H. Koenig, IBM J. Res. Dev. **8**, 234 (1964).
[27] J. L. Warren, J. L. Yarnell, G. Dolling, and R. A. Cowley, Phys. Rev. **158**, 805 (1967).